ANL/RE/CP--82357
Conf-940613--21

USE OF A VISCOELASTIC MODEL FOR THE SEISMIC RESPONSE OF BASE-ISOLATED BUILDINGS

R. Aziz Uras
Reactor Engineering Division
Argonne National Laboratory
Argonne, Illinois

ABSTRACT

Due to recent developments in elastomer technology, seismic isolation using elastomer bearings is rapidly becoming an acceptable design tool to enhance structural seismic margins and to protect people and equipment from earthquake damage. With proper design of isolators, high-energy seismic input motions are transformed into low-frequency, low energy harmonic motions and the accelerations acting on the isolated building are significantly reduced. Several alternatives exist for the modeling of the isolators. This study is concerned with the use of a viscoelastic model to predict the seismic response of base-isolated buildings. The in-house finite element computer code has been modified to incorporate a viscoelastic spring element, and several simulations are performed. Then, the computed results have been compared with the corresponding observed data recorded at the test facility.

INTRODUCTION

Seismic isolation using elastomer bearings can be adapted as a design tool to enhance the integrity of structures, and hence, to protect people and equipment from earthquake damage. With proper design of isolators, the fundamental frequency of the structure can be reduced to a value that is lower than the dominant frequencies of earthquake ground motions. Moreover, the accelerations transmitted to the superstructure can be greatly reduced through the damping mechanism provided in the isolators. Thus, high-energy seismic ground motions are transformed into low-frequency, low energy harmonic motions on the structure, and the structural accelerations acting on the isolated building are significantly reduced. In the USA, the use of seismic base-isolation has become an alternate strategy for advanced Liquid Metal-cooled Reactors (LMRs). Argonne National Laboratory (ANL) has been deeply involved in the development and implementation of seismic isolation for use in both nuclear facilities and civil structures for the past decade.

As a part of a joint study, the Argonne National Laboratory (ANL) and Shimizu Corporation of Japan mutually chose a seismic isolation system. Shimizu provided the test facility at Tohoku University in Sendai, Japan, while ANL supplied the isolator bearings to be installed at the test facility and performed most of the analysis needed for understanding each significant seismic event and correlating the results with appropriate laboratory tests. The isolator bearings are made of layers of elastomers and steel plates. Experimental results show that the elastomeric isolation bearing under sinusoidal loading exhibit a hysteresis loop. The slope of the hysteresis loop changes with the magnitude of the shear strain. For small shear strains, the slope of the hysteresis loop is fairly steep. When shear strain increases, the slope decreases with increased shear strain. This effect must be taken into account in the mathematical modeling so that the response of elastomeric bearings can be accurately predicted. This can be achieved through a viscoelastic model. The constitutive equation of the viscoelastic model uses five parameters which are to be derived from the experimental data obtained through elastomer coupon and isolator bearing tests. Numerical simulation of the individual isolator bearing response under sinusoidal loading using this viscoelastic model compares well with the experimental results. This model has been incorporated in the computer code, SISEC (Wang, et al., 1991). Seismic response of the test buildings under earthquake motion has been performed with this model. The computed results have been compared with the corresponding observed data recorded at the test facility.

During the test period for high shape factor-high damping rubber bearings, thirty-seven (37) earthquake motions were

recorded. This paper presents the detailed analysis on three of these earthquakes: one which had the largest amplitude of acceleration; one which had the longest time duration; and one which was the first earthquake that occurred after the installation of the bearings. Numerical simulations are performed with the ANL developed computer code, SISEC (Wang, et al., 1991). Each isolator is modeled with a viscoelastic spring element.

GENERAL DESCRIPTION OF ANL/SHIMIZU JOINT STUDY PROGRAM

Test Facility

The goal of the ANL/Shimizu Joint Program is to study the differences in behavior of base-isolated and ordinarily founded structures when subjected to earthquake loading. Shimizu Corporation has two test buildings, located at Tohoku University in Sendai, Japan. The base-isolated and the ordinary building stand side-by-side, and are full-sized three-story reinforced concrete structures. The superstructures were build as rigid frame structures with light-weight concrete panels used as outer walls. The dimensions of the two buildings are exactly the same, viz. 6 by 10 meters with a combined floor area of 180m^2. The additional space around the isolated building is intended to accommodate large displacements that may occur during large amplitude earthquakes.

The test buildings were founded on a relatively hard loam layer with gravel whose shear velocity is 310 m/sec (1017 ft/sec). Site predominant frequency obtained through micro-tremor observation is found to be about 4 Hz.

Base Isolation System

The isolation bearings used in the test facility were manufactured by Fluorocarbon Inc. (now FURON), USA. The bearing has 33 layers of high-damping rubber, 4.85 mm (0.19 in) per layer and 32 layers of steel shim plates, 1.9 mm (0.075 in) per layer. The diameter and the height of the bearing are 508 mm (20 in) and 284.2 mm (11 3/16 in), respectively. The bearing is designed to have a frequency of 0.75 Hz at 50% shear strain. Note the shear strain referred to is calculated from the total rubber height by excluding the thickness of steel shim plates. Vertical and horizontal stiffnesses of the bearing are 13.6x10^5 kgf/cm and 961 kgf/cm, respectively.

A total of eight (8) bearings were shipped to Shimizu Corporation, six of which were installed in the test building for earthquake observation and data acquisition. The remaining two bearings were reserved for laboratory testing for determining the dynamic characteristics of these base isolators.

The fundamental bearing characteristics in the horizontal direction are determined through a series of shearing tests. For example, the hysteretic loops of the bearing are determined from cycling loading tests. The equivalent stiffness, K_{eq} and the equivalent damping ratio, C_{eq}, given in Fig. 1, are calculated for different displacements using the following relations:

$$K_{eq} = (F^+ - F^-) / (d^+ - d^-) \quad (1)$$

and

$$C_{eq} = \Delta W / (2\pi W) \quad (2)$$

The shear modulus, G, and the shear strain, γ, of the bearing is thus obtained by

$$G = K_{eq} H_R / A \quad (3)$$

and

$$\gamma = d_H / H_R \quad (4)$$

where A, d_H and H_R are the cross-sectional area, the horizontal bearing shear displacement, and the total rubber height, respectively.

Earthquake Observation

The responses of both the isolated and the non-isolated buildings were recorded for all important earthquakes. A total of fifteen (15) accelerometers were placed at different locations on the two buildings and their surroundings. Four (4) accelerometers are placed on the ordinary building, three of them at the first floor level and the fourth one at the roof; the isolated building has seven (7) accelerometers: one is placed on the roof, three in the basement and three on the first floor. Four additional accelerometers are located in the vicinity of the twin buildings: two on the ground surface, one at 24 meters below the free surface and another one at 27 meters below the free surface.

During the test period, thirty-seven (37) earthquakes were recorded. Among all the observed earthquakes only ten (10) had a maximum ground acceleration of greater than 3 gal on the ground surface.

MATHEMATICAL MODELING

General Description

Three-dimensional space frames are employed to represent the superstructures of the ordinary building and isolated buildings. The beams, columns and girders of the buildings are represented by 3-D beam elements. No stiffness contribution is considered from the outer walls and partitions. However, the masses of these components are added into the appropriate nodal points. Three beam elements which also include the stiffness of the basement reinforced concrete wall are used to model each basement column for the ordinary building. In the case of the isolated building, two beam elements are used to model the reinforced concrete pedestals similar to the basement support columns in the ordinary building. Moreover, two spring elements are used to represent the behavior of the isolation bearing in the vertical and horizontal directions. The response in the vertical direction is represented by a linear spring since the stiffness in the vertical direction is about three orders of magnitude larger than that in the horizontal direction. The response in the

horizontal direction is represented by a viscoelastic spring element where rubber characteristics such as high damping and softening effects have been incorporated in the viscoelastic spring.

The finite element configuration used in the simulation is shown in Fig. 2 where the three locations labeled by numbers 111, 63, and 9 indicate the elevations of the basement, first floor and roof, respectively.

Viscoelastic Damage Model

With the increased use of elastomeric polymers in industrial applications such as isolation bearings, the importance of constitutive modeling of viscoelastic materials is more and more pronounced. A realistic representation of material behavior is essential for computer simulations to replicate the response observed in experiments. Figure 3 depicts a typical hysteresis curve obtained from horizontal shear tests of a bolted isolation bearing in which the axial load applied to the bearing is 926 kN (208 kips). As can be seen in Fig. 3, the shear stiffness decreases when shear strain increases. This softening effect has to be taken into account in the mathematical modeling.

Here, a fully three-dimensional finite-strain viscoelastic model developed by Simo and Taylor (1983, 1987) is employed to characterize the behavior of isolator bearings. In the Simo and Taylor model, the material is assumed to be isotropic in its virgin as well as in its deformed or damaged state. Volumetric and deviatoric responses are uncoupled over any range of deformation. The volumetric response is purely elastic. The proposed damage mechanism incorporates the softening behavior of rubber undergoing deformation (Mullin's effect). In the cyclic test, this translates into progressive degradation of the storage modulus with increasing maximum strain amplitude. The analytical hysteresis curve simulated by this proposed model is given in Fig. 4.

The constitutive relation for this viscoelastic model is comprised of five parameters derived from experimental findings. The softening response and the energy absorption characteristics of the rubber is identified from the hysteretic loops obtained through cyclic shear tests. This procedure is already explained in a previous section. Here, the important issues of the constitutive model are discussed. The equivalent stiffness for each hysteretic loop is computed using Eq. (1) (see Fig. 1). The effective shear modulus is determined from Eq. (3). They are then normalized with respect to the maximum value in the data set

$$G_i = G_i' / G_{max}' \qquad i=1,n \tag{7}$$

where n is the total number of data points (i.e. number of loops on the hysteresis curve), and

$$G_{max}' = \max \{G_i'\} \tag{8}$$

The maximum shear strain, ε_{max}, for each loop is calculated by

$$\varepsilon_{max} = d^* / H_R \tag{9}$$

where H_R is the total rubber height in the bearing.

The maximum shear strain is, then, plotted versus the normalized shear modulus. The following exponential function is used to fit a curve through the data points:

$$g(\varepsilon_{max}) = \beta + (1-\beta)*(1 - \exp(-\varepsilon_{max}/\alpha))/(\varepsilon_{max}/\alpha) \tag{10}$$

A graphical interpretation of Eq. (10) is depicted in Fig. 5, where β is the asymptote of function $g(\varepsilon_{max})$, α is the ε_{max} coordinate of the intersection of the asymptote with the tangent line drawn from $g(\varepsilon_{max})=1$. This exponential damage function is combined with the remaining three parameters to be extracted from the relaxation experiments forms the basis of the constitutive model. A simple exponential relaxation law provides values for the short-term shear modulus, G_0, the long-term shear modulus, G_∞, and the relaxation time constant, v:

$$G(t) = G_\infty + (G_\infty - G_0) \exp(-t/v) \tag{11}$$

where t denotes the time. Note that G_0 represents the curve-fitting parameter at t=0 whereas G_∞ corresponds to the value of the data point when $t \to \infty$.

For the bearings installed in Sendai test building, the values of G_0 and G_∞ are 2.66 MPa (386 psi) and 0.99 MPa (144 psi), respectively. The corresponding relaxation time constant is 0.45. Effective shear modulus and strain data revealed α and β are as 0.1 and 0.3, respectively.

RESULTS AND DISCUSSION

Out of the thirty-seven (37) earthquakes occurred during the test period, three (EQ.A, EQ.B, and EQ.C), are of significance for numerical simulation and comparison with observed data. Earthquake B has the largest amplitude accelerations. Earthquake C has the longest duration and a broad frequency spectrum. The range of frequencies in that earthquake indicates that the soil-structure interaction may be of importance. Earthquake A has the same order of magnitude as EQ.B and EQ.C. It occurred right after the installation of bearings, and the bearings were still in the virgin state. It is felt that the dynamic characteristics of the bearings can be obtained from the responses of the isolated building under those three earthquakes.

Comparisons among the observed response and the simulation results obtained using the viscoelastic spring model are presented. In order to emphasize the effectiveness of the viscoelastic model for isolation bearings, and to minimize the influence of the superstructure, the detailed analysis in given only for the first floor.

Comparison of Results for Earthquake A

In the longitudinal direction, the input record has one dominant frequency of 2.80 Hz (Fig. 6). The maximum response amplitude obtained from simulations with viscoelastic model for the first floor is only 8% smaller than the observed one. The frequency spectrum derived from the time history computations through FFT for the viscoelastic model gives the response

frequency of 2.40 Hz for the first floor which is exactly the same as the observed value.

In the transverse direction, comparably large peaks with the dominant one located at 2.57 Hz are encountered in the input record, see Fig. 7. The first floor maximum response amplitude of the viscoelastic simulations is 11% smaller than that of the observed, and the response frequencies are 2.30 Hz and 2.37 Hz, respectively.

Comparison of Results for Earthquake B

In the longitudinal direction, similar to Earthquake A, the input acceleration of the Earthquake B has one dominant frequency of 2.23 Hz (Fig. 8). The maximum response amplitude for the first floor of the viscoelastic model is 25% greater than the observed one. The frequency spectrum of the viscoelastic model derived from the time history computations through FFT yields a response frequency of 2.23 Hz for the first floor whereas the observed frequency is 2.27 Hz. It should be noted that a comparably large peak is found at 2.40 Hz both in the observed and computed frequency spectra.

In the transverse direction, comparably large peaks (dominant frequency at 2.57 Hz) are encountered in the input record (Fig. 9). The first floor maximum response amplitude from the viscoelastic model is 15% smaller than that of the observed. The computed frequency for the first floor is 2.30 Hz. However, the observed data yields 2.07 Hz for the first floor with several closely-spaced frequencies in 2.07-2.42 Hz range.

Comparison of Results for Earthquake C

In the longitudinal direction, unlike Earthquake A and B, the input record for Earthquake C reveals a broad spectrum with closely spaced frequencies in 1.09-2.15 Hz range. The largest amplitude frequency is 1.28 Hz (Fig. 10). The maximum response amplitude obtained with the viscoelastic model simulations for the first floor is 35% larger than the observed one as a result of the broad input spectrum. The frequency spectrum obtained from computer simulations yields a response frequency of 2.39 Hz whereas the observed data reveals a frequency of 2.67 Hz. It is noted that closely spaced frequencies are found both in the observed (2.2-2.8 Hz) and computed (2.2-2.6 Hz) frequency spectra.

Similarly, in the transverse direction, the input record for the Earthquake C reveals a broad spectrum in 1.00-2.20 Hz range with a dominant frequency of 1.59 Hz (Fig. 11). The first floor maximum response amplitude with the viscoelastic model is 28% larger than that of the observed value. The computed and observed frequencies are 2.20 Hz and 2.36 Hz, respectively.

CONCLUSIONS

The comparison of results shows that the viscoelastic model can predict the actual behavior of highly-filled rubber material used in isolator bearings rather accurately. However, the effectiveness of this model is somewhat dependent on the input spectrum. When the spectrum of the input motion has a clear dominant frequency, the simulation results are in excellent agreement with the experimentally observed data. When the input motion has a wide range of frequencies, and no visible dominant frequency exists in the spectrum, the maximum response predicted by the model is shown to be off about 30%.

One major drawback of the viscoelastic model is that its implementation requires the availability of two types of test data: cyclic shear and relaxation tests. However, it is highly recommended that the viscoelastic model be used in the future seismic response analysis if all the required data of cyclic shear and relaxation tests are available.

ACKNOWLEDGMENT

Work supported by the National Science Foundation, Agreement No. CES-8800871.

REFERENCES

Simo, J. C. and Taylor, R. L., 1983, "A Simple Three Dimensional Model Accounting for Damage Effects," Technical Report UCB/SESM/83-10, Department of Civil Engineering, University of California, Berkeley, CA.

Simo, J. C., 1987, "On a Fully Three-Dimensional Finite-Strain Viscoelastic Damage Model: Formulation and Computational Aspects," *Computer Methods in Applied Mechanics and Engineering*, Vol. 60, pp. 153-173.

Wang, C. Y., et al., 1991, "System Response Analyses of Base-isolated Structure to Earthquake Ground Motions," *Proceedings, 11th International Conference on Structural Mechanics in Reactor Technology (SMiRT-11)*, paper K26/6, Tokyo, Japan.

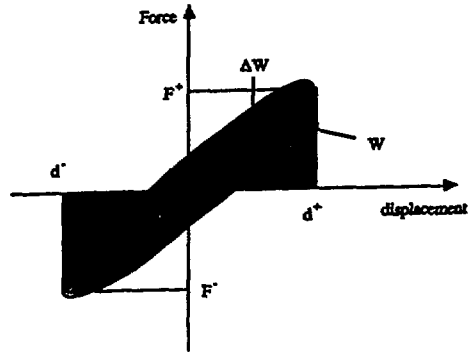

FIG 1. COMPUTATION OF THE EQUIVALENT STIFFNESS AND DAMPING

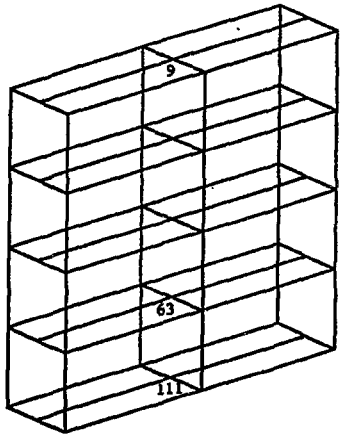

ordinary building

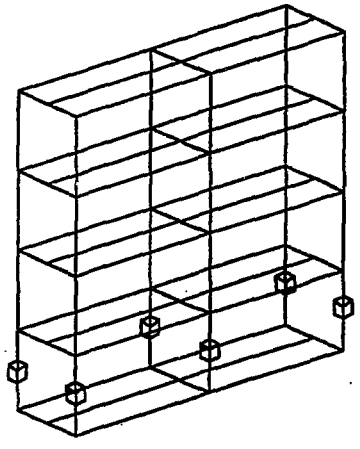

base-isolated building

›ring-damper system to model base isolation

2. MODELS FOR THE ORDINARY AND BASE-ISOLATED BUILDINGS

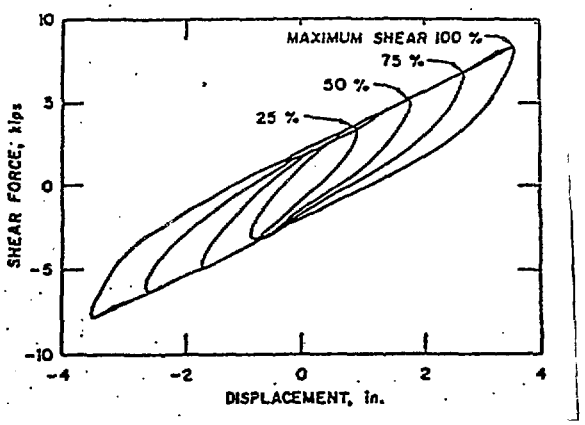

FIG. 3. HYSTERESIS CURVES OBTAINED FROM HORIZONTAL SHEAR TEST

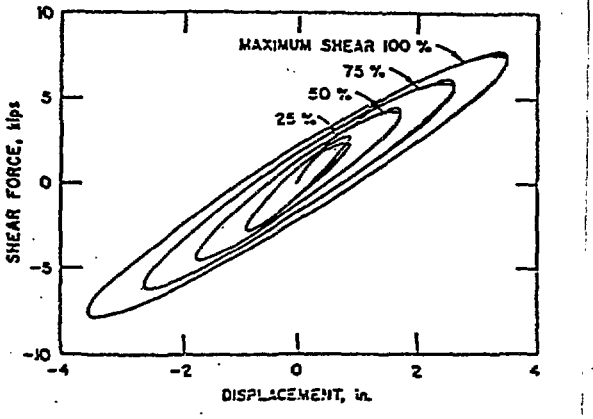

FIG. 4. ANALYTICALLY SIMULATED HYSTERESIS CURVES

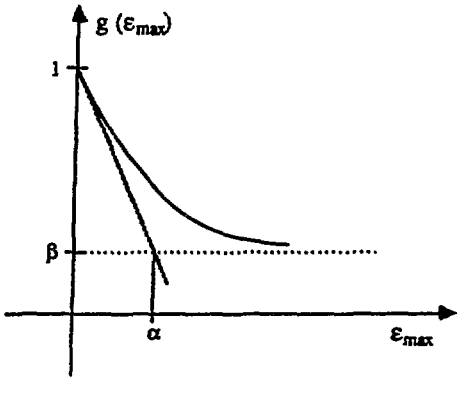

FIG. 5. GEOMETRICAL MEANING OF α AND β

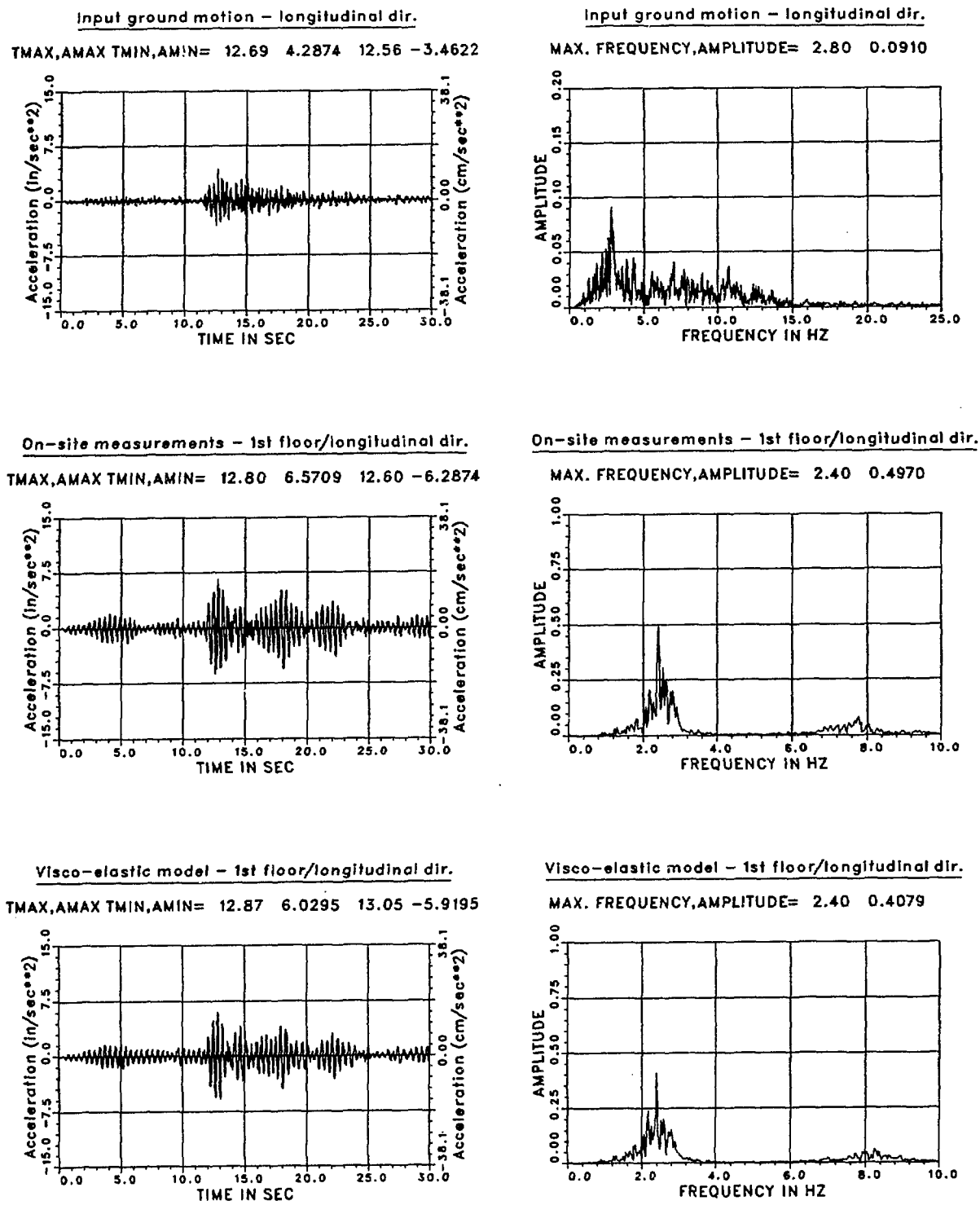

FIG. 6. COMPARISONS FOR EARTHQUAKE A IN THE LONGITUDINAL DIRECTION AT THE FIRST FLOOR

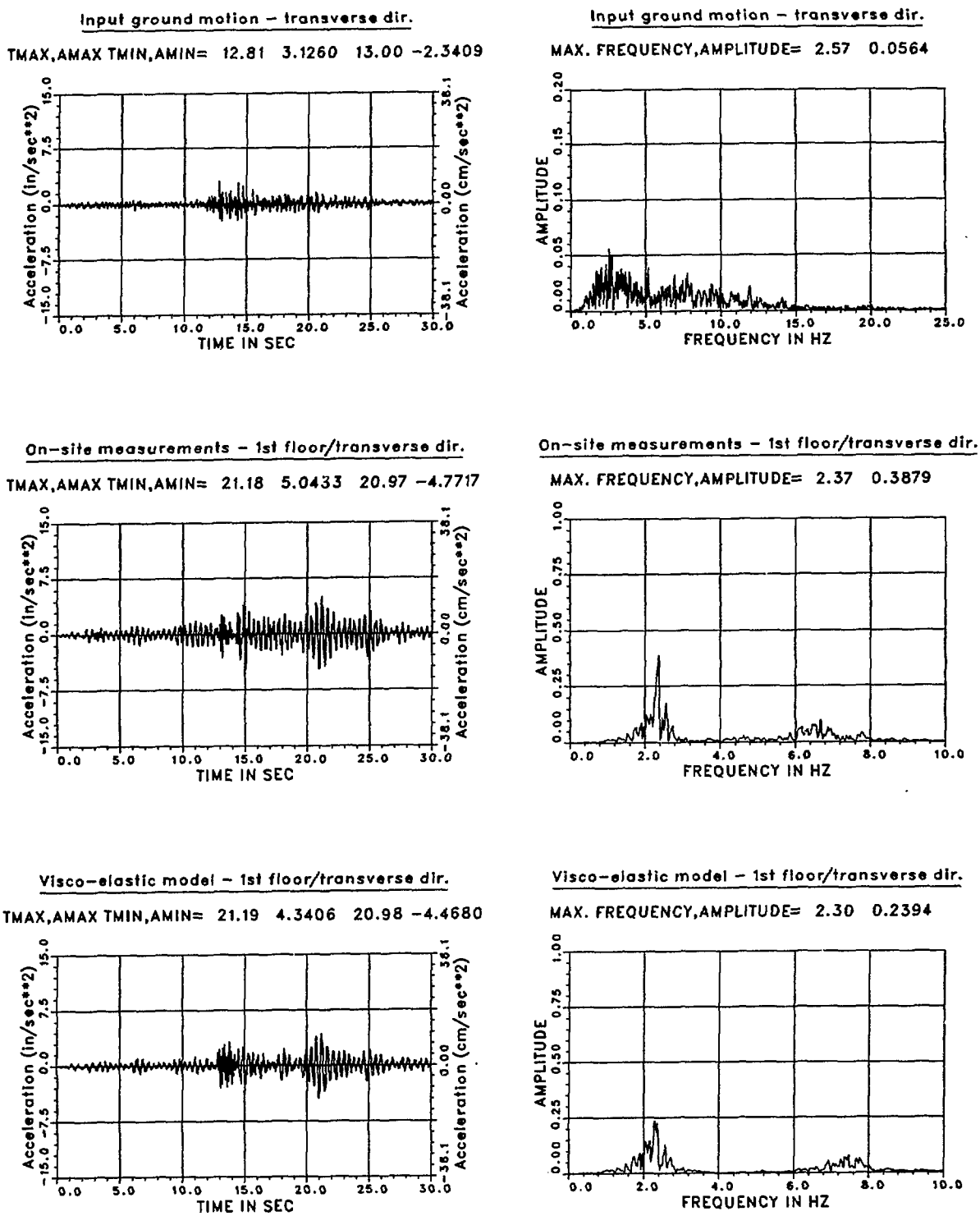

FIG. 7. COMPARISONS FOR EARTHQUAKE A IN THE TRANSVERSE DIRECTION AT THE FIRST FLOOR

Input ground motion – longitudinal dir.

TMAX,AMAX TMIN,AMIN= 2.09 7.4331 1.87 -11.5512

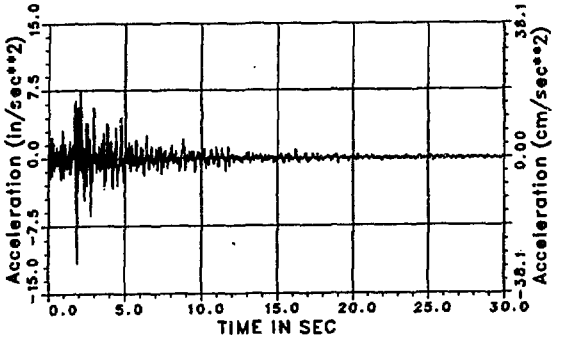

Input ground motion – longitudinal dir.

MAX. FREQUENCY,AMPLITUDE= 2.23 0.1209

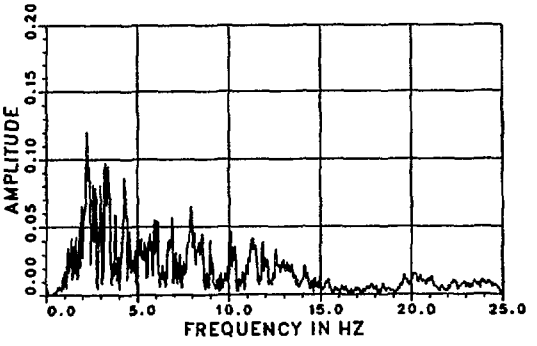

On-site measurements – 1st floor/longitudinal dir.

TMAX,AMAX TMIN,AMIN= 2.21 12.9685 2.41 -13.3780

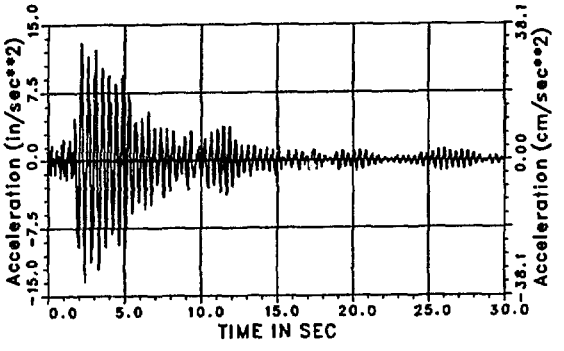

On-site measurements – 1st floor/longitudinal dir.

MAX. FREQUENCY,AMPLITUDE= 2.27 0.6167

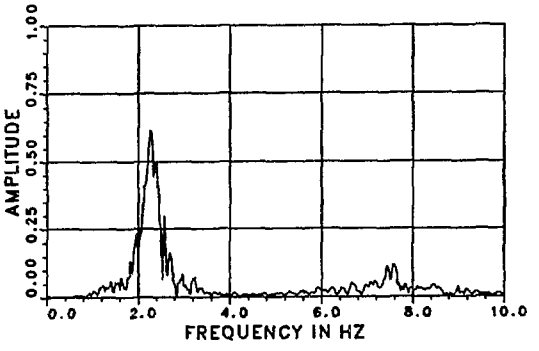

Visco-elastic model – 1st floor/longitudinal dir.

TMAX,AMAX TMIN,AMIN= 3.08 16.6840 2.89 -14.9955

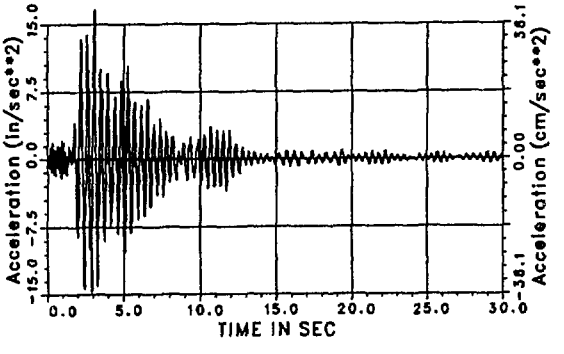

Visco-elastic model – 1st floor/longitudinal dir.

MAX. FREQUENCY,AMPLITUDE= 2.23 0.7622

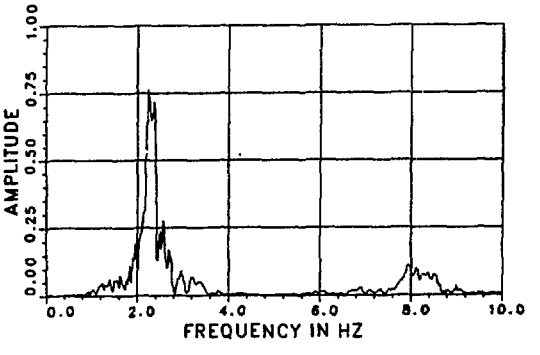

FIG. 8. COMPARISONS FOR EARTHQUAKE B IN THE LONGITUDINAL DIRECTION AT THE FIRST FLOOR

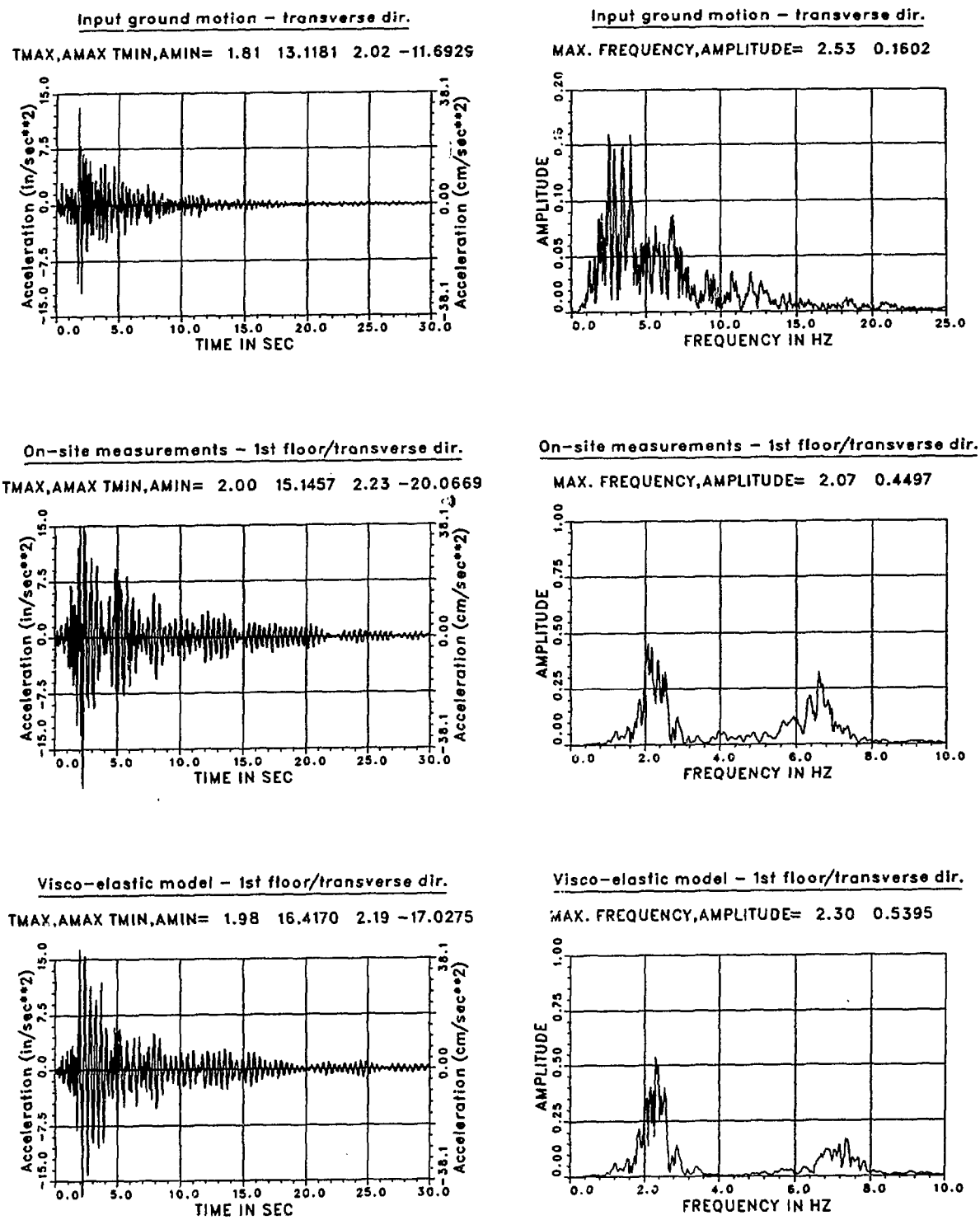

FIG. 9. COMPARISONS FOR EARTHQUAKE B IN THE TRANSVERSE DIRECTION AT THE FIRST FLOOR

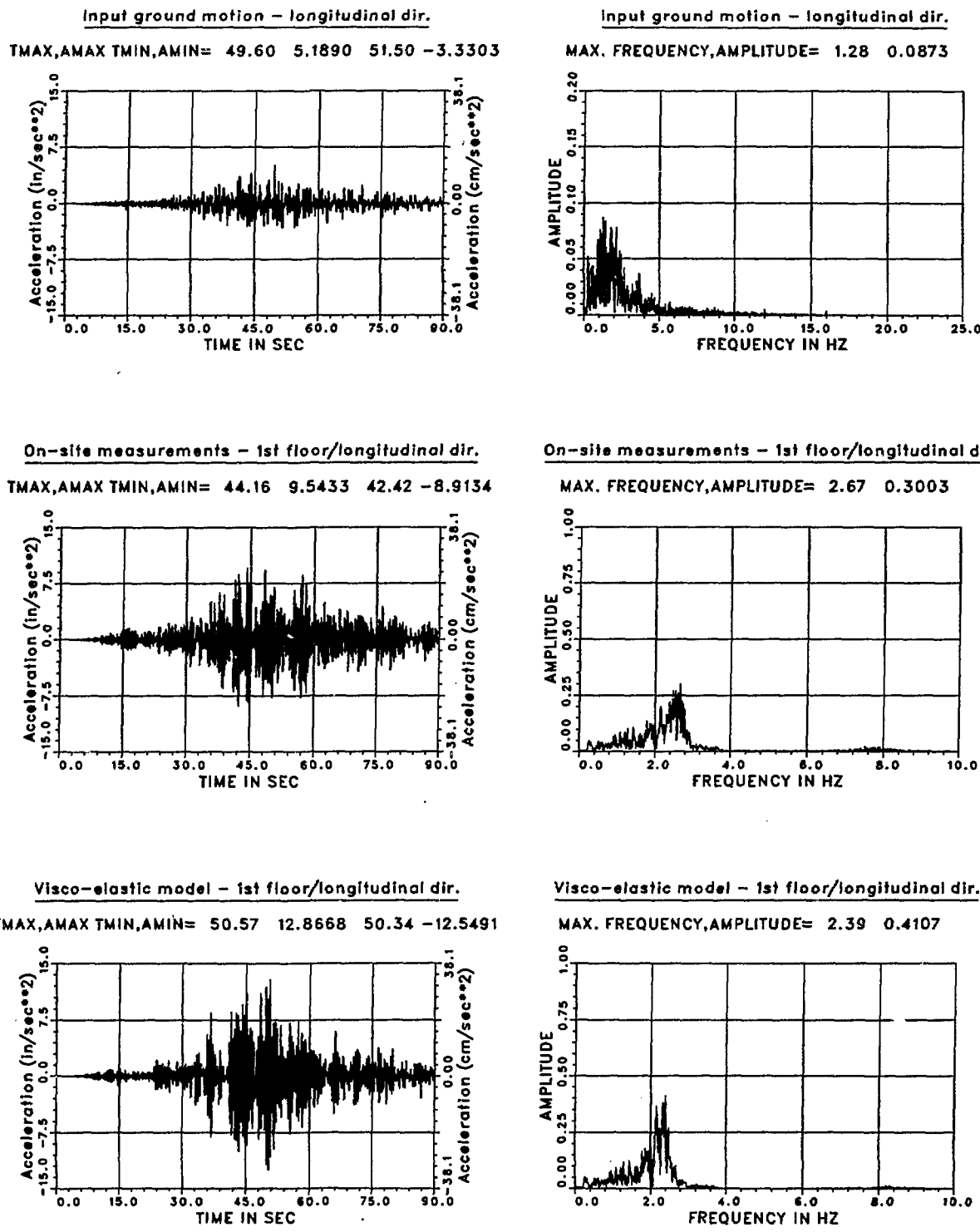

FIG. 10. COMPARISONS FOR EARTHQUAKE C IN THE LONGITUDINAL DIRECTION AT THE FIRST FLOOR

Input ground motion – transverse dir.

TMAX,AMAX TMIN,AMIN= 53.10 3.8114 52.74 -4.1535

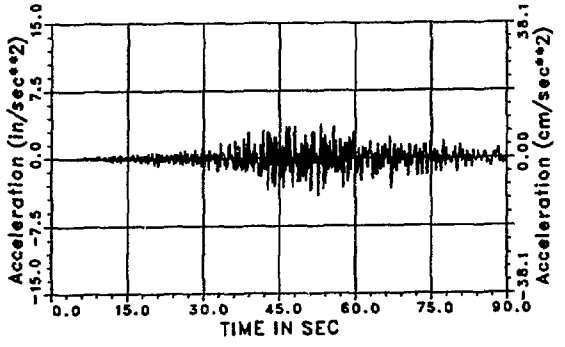

Input ground motion – transverse dir.

MAX. FREQUENCY,AMPLITUDE= 1.59 0.1055

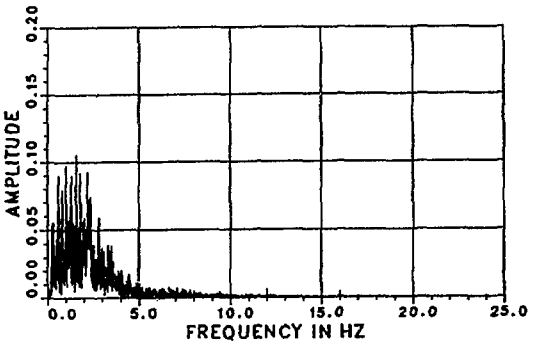

On-site measurements – 1st floor/transverse dir.

TMAX,AMAX TMIN,AMIN= 48.13 10.1339 54.32 -9.7520

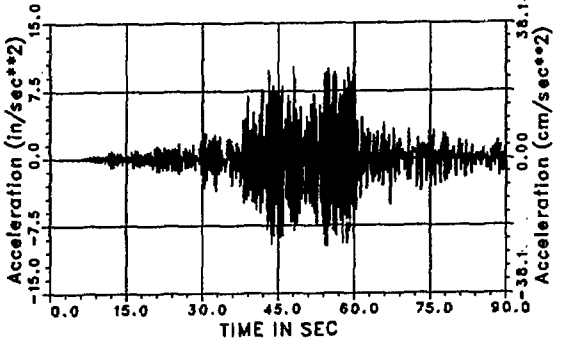

On-site measurements – 1st floor/transverse dir.

MAX. FREQUENCY,AMPLITUDE= 2.36 0.5530

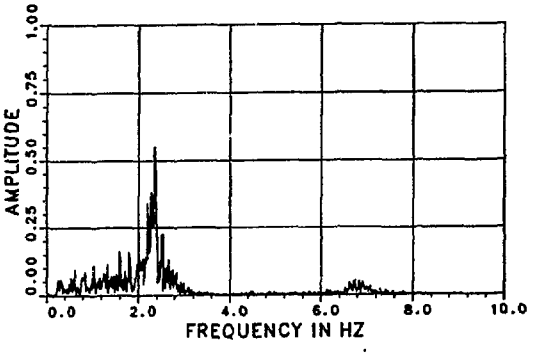

Visco-elastic model – 1st floor/transverse dir.

TMAX,AMAX TMIN,AMIN= 44.50 12.5069 44.26 -12.9893

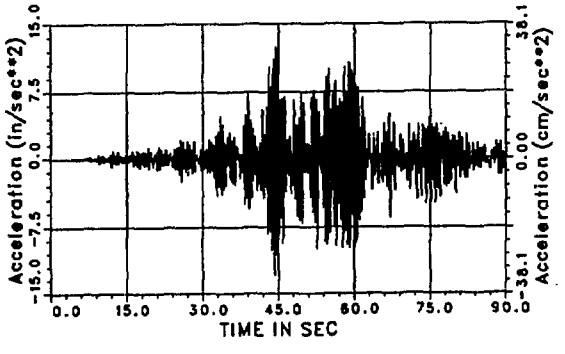

Visco-elastic model – 1st floor/transverse dir.

MAX. FREQUENCY,AMPLITUDE= 2.20 0.6189

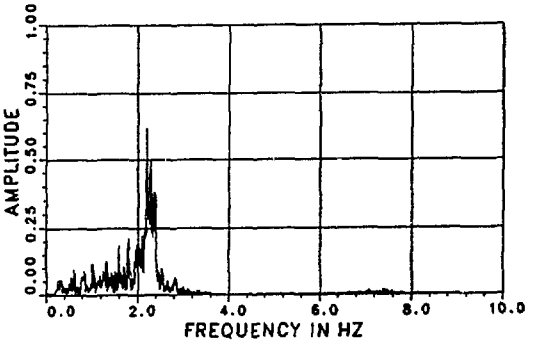

FIG. 11. COMPARISONS FOR EARTHQUAKE C IN THE TRANSVERSE DIRECTION AT THE FIRST FLOOR